

# EMPIRICAL GROUND MOTION MODEL FOR SHALLOW CRUSTAL EARTHQUAKES IN ACTIVE TECTONIC ENVIRONMENTS DEVELOPED FOR THE NGA PROJECT

K.W. Campbell<sup>1</sup> and Y. Bozorgnia<sup>2</sup>

<sup>1</sup> Vice President, ABS Consulting (EQECAT), Beaverton, Oregon, USA

<sup>2</sup> Associate Director, PEER, University of California, Berkeley, California, USA

Email: [kcampbell@eqecat.com](mailto:kcampbell@eqecat.com), [yousef@berkeley.edu](mailto:yousef@berkeley.edu)

## ABSTRACT

We present a new empirical ground motion model for PGA, PGV, PGD and 5% damped linear elastic response spectra for periods ranging from 0.01–10 s. The model was developed as part of the PEER Next Generation Attenuation (NGA) project. We used a subset of the PEER NGA database for which we excluded recordings and earthquakes that were believed to be inappropriate for estimating free-field ground motions from shallow earthquake mainshocks in active tectonic regimes. We developed relations for both the median and standard deviation of the geometric mean horizontal component of ground motion that we consider to be valid for magnitudes ranging from 4.0 up to 7.5–8.5 (depending on fault mechanism) and distances ranging from 0–200 km. The model explicitly includes the effects of magnitude saturation, magnitude-dependent attenuation, style of faulting, rupture depth, hanging-wall geometry, linear and nonlinear site response, 3-D basin response, and inter-event and intra-event variability. Soil nonlinearity causes the intra-event standard deviation to depend on the amplitude of PGA on reference rock rather than on magnitude, which leads to a decrease in aleatory uncertainty at high levels of ground shaking for sites located on soil.

**KEYWORDS:** Attenuation, Ground Motion Prediction, Response Spectra, Active Tectonic Regions

## 1. INTRODUCTION

The empirical ground motion model (also referred to as an attenuation relation or ground motion prediction equation) presented in this paper represents the culmination of a four-year multidisciplinary study sponsored by the Pacific Earthquake Engineering Research Center (PEER) referred to as the Next Generation Attenuation (NGA) Ground Motion Project (Power et al., 2008). This new ground motion model supersedes our existing ground motion models for peak ground velocity (PGV) (Campbell, 1997) and peak ground acceleration (PGA) and 5% damped pseudo-absolute response spectral acceleration (PSA) (Campbell and Bozorgnia, 2003). Our NGA model represents a major advancement in ground motion prediction made possible by the extensive update of the PEER strong motion database and the supporting studies on 1-D ground motion simulation, 1-D site response, and 3-D basin response sponsored by the NGA project. This paper provides a brief description of the database, functional forms, and analyses that went into the development of the new NGA ground motion model. Additional documentation is given in Campbell and Bozorgnia (2007, 2008).

## 2. DATABASE

The database used for this study is a subset of the updated PEER strong motion database (Chiou et al., 2008). The general criteria that we used to select this subset was intended to meet our requirements that (1) the earthquake be located within the shallow continental lithosphere (i.e., the Earth's crust) in a region considered to be tectonically active, (2) that the recording be located at or near ground level and exhibit no known embedment or topographic effects, (3) that the earthquake have enough recordings to reliably represent the mean horizontal ground motion (especially for small-magnitude events), and (4) that the earthquake or the recording be considered reliable according to criteria set forth in Campbell and Bozorgnia (2007).

Application of the above criteria resulted in the selection of 1561 recordings from 64 earthquakes with moment magnitudes ( $M$ ) ranging from 4.3–7.9 and rupture distances ( $R_{RUP}$ ) ranging from 0.1–199 km. Table 1 of Campbell and Bozorgnia (2008) presents a summary of these earthquakes. A complete list of the selected earthquakes and recording stations are given in Appendix A of Campbell and Bozorgnia (2007). The distribution of the recordings with respect to magnitude and distance is shown in Fig. 1.

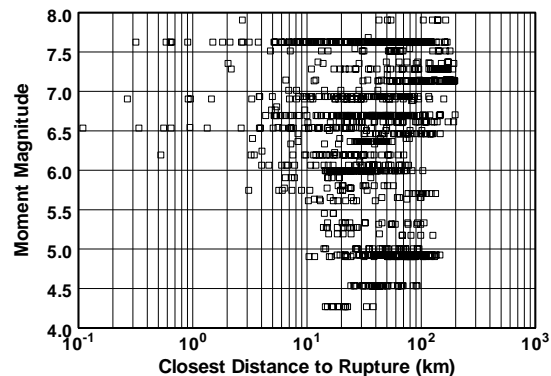


Figure 1. Database used in the analysis.

### 3. GROUND MOTION MODEL

The functional forms used to define our NGA model were either developed by us or evaluated from those available from the literature or proposed during the NGA project. Final functional forms were selected according to (1) their sound seismological basis; (2) their unbiased residuals; (3) their ability to be extrapolated to values of magnitude, distance, and other explanatory variables that are important for use in engineering and seismology; and (4) their simplicity, although this latter consideration was not an overriding factor. The third criterion was the most difficult to achieve because the data did not always allow the functional forms of some explanatory variables to be developed empirically. In such cases, theoretical constraints were used to define the functional forms based on supporting studies sponsored by the NGA project (Power et al., 2008).

During the model development phase of the study, regression analyses were performed in two stages for a limited set of oscillator periods ( $T$ ) using a two-stage nonlinear regression procedure. In Stage 1, the mathematical terms involving individual recordings (the intra-event terms) were fit by the method of nonlinear least squares using all of the recordings. In Stage 2, the mathematical terms common to all recordings of a specific earthquake (the inter-event terms) were fit by the method of weighted least squares using the event terms from Stage 1 as the “data”. Each event term was assigned a weight that was inversely proportional to its calculated variance from Stage 1. This two-stage analysis allowed us to decouple the intra-event and inter-event terms, which stabilized the regression analysis and allowed us to independently evaluate and model magnitude scaling effects at large magnitudes. Once the functional forms for all of the mathematical terms were established, a series of iterative random-effects regression analyses were performed for the entire range of periods in order to derive a smoothed set of model coefficients and to calculate the final values of the inter-event and intra-event standard deviations.

#### 3.1. Definition of Ground Motion Component

The ground motion component used in our NGA model is not the traditional geometric mean of the two “as-recorded” horizontal components that has been used in past studies. The principle drawback of the old geometric mean is its dependence on the orientation of the sensors as installed in the field. The new geometric mean, referred to as “GMRotI50” by Boore et al. (2006), is independent of both sensor orientation and oscillator period and, as a result, represents a more robust horizontal ground motion component. It was found to have a value that is on average within a few percent of the old geometric mean. In some engineering applications it is

necessary to calculate the median and aleatory uncertainty of the arbitrary horizontal component (Baker and Cornell, 2006). The median estimate of this component is equivalent to the median estimate of the traditional geometric mean. However, as discussed latter in the paper, its variance must be increased by the variance of the component-to-component variability between the two horizontal components of the recording. The relationship between the new geometric mean and other horizontal ground motion components, such as the maximum arbitrary (as-recorded) horizontal component, the maximum rotated horizontal component, and the strike-normal component can be found in Campbell and Bozorgnia (2007, 2008) and references therein.

### 3.2. Median Ground Motion Model

The median estimate of ground motion can be calculated from the general equation

$$\ln Y_{ij} = f_{mag} + f_{dis} + f_{flt} + f_{hng} + f_{site} + f_{sed} \quad (3.1)$$

where

$$f_{mag} = \begin{cases} c_0 + c_1 \mathbf{M}; & \mathbf{M} \leq 5.5 \\ c_0 + c_1 \mathbf{M} + c_2 (\mathbf{M} - 5.5); & 5.5 < \mathbf{M} \leq 6.5 \\ c_0 + c_1 \mathbf{M} + c_2 (\mathbf{M} - 5.5) + c_3 (\mathbf{M} - 6.5); & \mathbf{M} > 6.5 \end{cases} \quad (3.2)$$

$$f_{dis} = (c_4 + c_5 \mathbf{M}) \ln \left( \sqrt{R_{RUP}^2 + c_6^2} \right) \quad (3.3)$$

$$f_{flt} = c_7 F_{RV} f_{flt,Z} + c_8 F_{NM} \quad (3.4)$$

$$f_{flt,Z} = \begin{cases} Z_{TOR}; & Z_{TOR} < 1 \\ 1; & Z_{TOR} \geq 1 \end{cases} \quad (3.5)$$

$$f_{hng} = c_9 f_{hng,R} f_{hng,M} f_{hng,Z} f_{hng,\delta} \quad (3.6)$$

$$f_{hng,R} = \begin{cases} 1; & R_{JB} = 0 \\ \left[ \max \left( R_{RUP}, \sqrt{R_{JB}^2 + 1} \right) - R_{JB} \right] / \max \left( R_{RUP}, \sqrt{R_{JB}^2 + 1} \right); & R_{JB} > 0, Z_{TOR} < 1 \\ (R_{RUP} - R_{JB}) / R_{RUP}; & R_{JB} > 0, Z_{TOR} \geq 1 \end{cases} \quad (3.7)$$

$$f_{hng,M} = \begin{cases} 0; & \mathbf{M} \leq 6.0 \\ 2(\mathbf{M} - 6.0); & 6.0 < \mathbf{M} < 6.5 \\ 1; & \mathbf{M} \geq 6.5 \end{cases} \quad (3.8)$$

$$f_{hng,Z} = \begin{cases} 0; & Z_{TOR} \geq 20 \\ (20 - Z_{TOR}) / 20; & 0 \leq Z_{TOR} < 20 \end{cases} \quad (3.9)$$

$$f_{hng,\delta} = \begin{cases} 1; & \delta \leq 70 \\ (90 - \delta) / 20; & \delta > 70 \end{cases} \quad (3.10)$$

$$f_{site} = \begin{cases} c_{10} \ln\left(\frac{V_{S30}}{k_1}\right) + k_2 \left\{ \ln\left[A_{1100} + c\left(\frac{V_{S30}}{k_1}\right)^n\right] - \ln[A_{1100} + c] \right\}; & V_{S30} < k_1 \\ (c_{10} + k_2 n) \ln\left(\frac{V_{S30}}{k_1}\right); & k_1 \leq V_{S30} < 1100 \\ (c_{10} + k_2 n) \ln\left(\frac{1100}{k_1}\right); & V_{S30} \geq 1100 \end{cases} \quad (3.11)$$

$$f_{sed} = \begin{cases} c_{11}(Z_{2.5} - 1); & Z_{2.5} < 1 \\ 0; & 1 \leq Z_{2.5} \leq 3 \\ c_{12}k_3 e^{-0.75} [1 - e^{-0.25(Z_{2.5}-3)}]; & Z_{2.5} > 3 \end{cases} \quad (3.12)$$

In the above equations,  $Y_{ij}$  is the median estimate of the geometric mean horizontal component (GMRot150) of PGA (g), PGV (cm/s), PGD (cm) or PSA (g) for site  $j$  of event  $i$ ;  $\mathbf{M}$  is moment magnitude;  $R_{RUP}$  is the closest distance to the coseismic rupture plane (km);  $R_{JB}$  is the closest distance to the surface projection of the coseismic rupture plane (km);  $F_{RV}$  is an indicator variable representing reverse and reverse-oblique faulting, where  $F_{RV} = 1$  for  $30^\circ < \lambda < 150^\circ$ ,  $F_{RV} = 0$  otherwise, and  $\lambda$  is the rake defined as the average angle of slip measured in the plane of rupture between the strike direction and the slip vector;  $F_{NM}$  is an indicator variable representing normal and normal-oblique faulting, where  $F_{NM} = 1$  for  $-150^\circ < \lambda < -30^\circ$  and  $F_{NM} = 0$  otherwise;  $Z_{TOR}$  is the depth to the top of the coseismic rupture plane (km);  $\delta$  is the dip of the rupture plane ( $^\circ$ );  $V_{S30}$  is the time-averaged shear-wave velocity in the top 30 m of the site profile (m/s);  $A_{1100}$  is the median estimate of PGA on a reference rock outcrop with  $V_{S30} = 1100$  m/s (g); and  $Z_{2.5}$  is the depth to the 2.5 km/s shear-wave velocity horizon, typically referred to as basin or sediment depth (km). The empirical coefficients  $c_i$  and the theoretical coefficients  $c$ ,  $n$  and  $k_i$  are listed in Table 1. When  $PSA < PGA$  and  $T \leq 0.25$  s, PSA should be set equal to PGA to be consistent with the definition of pseudo-absolute acceleration.

Table 1. Coefficients for the median ground motion model

$T$ (s)	$c_0$	$c_1$	$c_2$	$c_3$	$c_4$	$c_5$	$c_6$	$c_7$	$c_8$
0.010	-1.715	0.500	-0.530	-0.262	-2.118	0.170	5.60	0.280	-0.120
0.020	-1.680	0.500	-0.530	-0.262	-2.123	0.170	5.60	0.280	-0.120
0.030	-1.552	0.500	-0.530	-0.262	-2.145	0.170	5.60	0.280	-0.120
0.050	-1.209	0.500	-0.530	-0.267	-2.199	0.170	5.74	0.280	-0.120
0.075	-0.657	0.500	-0.530	-0.302	-2.277	0.170	7.09	0.280	-0.120
0.10	-0.314	0.500	-0.530	-0.324	-2.318	0.170	8.05	0.280	-0.099
0.15	-0.133	0.500	-0.530	-0.339	-2.309	0.170	8.79	0.280	-0.048
0.20	-0.486	0.500	-0.446	-0.398	-2.220	0.170	7.60	0.280	-0.012
0.25	-0.890	0.500	-0.362	-0.458	-2.146	0.170	6.58	0.280	0.000
0.30	-1.171	0.500	-0.294	-0.511	-2.095	0.170	6.04	0.280	0.000
0.40	-1.466	0.500	-0.186	-0.592	-2.066	0.170	5.30	0.280	0.000
0.50	-2.569	0.656	-0.304	-0.536	-2.041	0.170	4.73	0.280	0.000
0.75	-4.844	0.972	-0.578	-0.406	-2.000	0.170	4.00	0.280	0.000
1.0	-6.406	1.196	-0.772	-0.314	-2.000	0.170	4.00	0.255	0.000
1.5	-8.692	1.513	-1.046	-0.185	-2.000	0.170	4.00	0.161	0.000
2.0	-9.701	1.600	-0.978	-0.236	-2.000	0.170	4.00	0.094	0.000
3.0	-10.556	1.600	-0.638	-0.491	-2.000	0.170	4.00	0.000	0.000
4.0	-11.212	1.600	-0.316	-0.770	-2.000	0.170	4.00	0.000	0.000
5.0	-11.684	1.600	-0.070	-0.986	-2.000	0.170	4.00	0.000	0.000

7.5	-12.505	1.600	-0.070	-0.656	-2.000	0.170	4.00	0.000	0.000
10.0	-13.087	1.600	-0.070	-0.422	-2.000	0.170	4.00	0.000	0.000
PGA	-1.715	0.500	-0.530	-0.262	-2.118	0.170	5.60	0.280	-0.120
PGV	0.954	0.696	-0.309	-0.019	-2.016	0.170	4.00	0.245	0.000
PGD	-5.270	1.600	-0.070	0.000	-2.000	0.170	4.00	0.000	0.000

$T (s)$	$c_9$	$c_{10}$	$c_{11}$	$c_{12}$	$k_1$	$k_2$	$k_3$	$c$	$n$
0.010	0.490	1.058	0.040	0.610	865	-1.186	1.839	1.88	1.18
0.020	0.490	1.102	0.040	0.610	865	-1.219	1.840	1.88	1.18
0.030	0.490	1.174	0.040	0.610	908	-1.273	1.841	1.88	1.18
0.050	0.490	1.272	0.040	0.610	1054	-1.346	1.843	1.88	1.18
0.075	0.490	1.438	0.040	0.610	1086	-1.471	1.845	1.88	1.18
0.10	0.490	1.604	0.040	0.610	1032	-1.624	1.847	1.88	1.18
0.15	0.490	1.928	0.040	0.610	878	-1.931	1.852	1.88	1.18
0.20	0.490	2.194	0.040	0.610	748	-2.188	1.856	1.88	1.18
0.25	0.490	2.351	0.040	0.700	654	-2.381	1.861	1.88	1.18
0.30	0.490	2.460	0.040	0.750	587	-2.518	1.865	1.88	1.18
0.40	0.490	2.587	0.040	0.850	503	-2.657	1.874	1.88	1.18
0.50	0.490	2.544	0.040	0.883	457	-2.669	1.883	1.88	1.18
0.75	0.490	2.133	0.077	1.000	410	-2.401	1.906	1.88	1.18
1.0	0.490	1.571	0.150	1.000	400	-1.955	1.929	1.88	1.18
1.5	0.490	0.406	0.253	1.000	400	-1.025	1.974	1.88	1.18
2.0	0.371	-0.456	0.300	1.000	400	-0.299	2.019	1.88	1.18
3.0	0.154	-0.820	0.300	1.000	400	0.000	2.110	1.88	1.18
4.0	0.000	-0.820	0.300	1.000	400	0.000	2.200	1.88	1.18
5.0	0.000	-0.820	0.300	1.000	400	0.000	2.291	1.88	1.18
7.5	0.000	-0.820	0.300	1.000	400	0.000	2.517	1.88	1.18
10.0	0.000	-0.820	0.300	1.000	400	0.000	2.744	1.88	1.18
PGA	0.490	1.058	0.040	0.610	865	-1.186	1.839	1.88	1.18
PGV	0.358	1.694	0.092	1.000	400	-1.955	1.929	1.88	1.18
PGD	0.000	-0.820	0.300	1.000	400	0.000	2.744	1.88	1.18

### 3.3. Aleatory Uncertainty Model

Consistent with the random-effects regression analysis that was used to derive the median ground motion model, the aleatory uncertainty model is defined by the equation

$$\ln y_{ij} = \ln Y_{ij} + \eta_i + \varepsilon_{ij} \quad (3.13)$$

where  $\eta_i$  is the inter-event residual for event  $i$  and  $y$ ,  $y_{ij}$  and  $\varepsilon_{ij}$  are the predicted value, the observed value, and the intra-event residual for recording  $j$  of event  $i$ . The independent normally distributed variables  $\eta_i$  and  $\varepsilon_{ij}$  have zero means and an estimated inter-event standard deviation ( $\tau$ ) and intra-event standard deviation ( $\sigma$ ) given by the equations

$$\tau = \tau_{\ln Y} \quad (3.14)$$

$$\sigma = \sqrt{\sigma_{\ln Y_B}^2 + \sigma_{\ln A_F}^2 + \alpha^2 \sigma_{\ln A_B}^2 + 2\alpha\rho\sigma_{\ln Y_B}\sigma_{\ln A_B}} \quad (3.15)$$

which result in a total standard deviation of

$$\sigma_T = \sqrt{\sigma^2 + \tau^2} \quad (3.16)$$

In the above equations,  $\tau_{\ln Y}$  is the standard deviation of the inter-event residuals;  $\sigma_{\ln Y_B} = (\sigma_{\ln Y}^2 - \sigma_{\ln A_F}^2)^{1/2}$  is the estimated standard deviation of ground motion at the base of the site profile;  $\sigma_{\ln Y}$  is the standard deviation of the intra-event residuals;  $\sigma_{\ln A_F}$  is the estimated standard deviation of the logarithm of the site amplification factor  $f_{site}$  assuming linear site response;  $\sigma_{\ln A_B} = (\sigma_{\ln PGA}^2 - \sigma_{\ln A_F}^2)^{1/2}$  is the estimated standard deviation of PGA on reference rock at the base of the site profile;  $\sigma_{\ln PGA}$  is the standard deviation of PGA;  $\rho$  is the correlation coefficient between the intra-event residuals of the ground motion parameter of interest and PGA; and  $\alpha$  is the linearized functional relationship between  $f_{site}$  and  $\ln A_{1100}$ , which is estimated from the partial derivative

$$\alpha = \frac{\partial f_{site}}{\partial \ln A_{1100}} = \begin{cases} k_2 A_{1100} \left\{ \left[ A_{1100} + c (V_{S30}/k_1)^n \right]^{-1} - (A_{1100} + c)^{-1} \right\} & V_{S30} < k_1 \\ 0 & V_{S30} \geq k_1 \end{cases} \quad (3.17)$$

where the coefficients  $k_1$ ,  $k_2$ ,  $c$  and  $n$  are listed in Table 1. The standard deviations  $\tau_{\ln Y}$ ,  $\sigma_{\ln Y}$ ,  $\sigma_{\ln PGA}$  and  $\sigma_{\ln A_F}$  and the correlation coefficient  $\rho$  are listed in Table 2. Details summarizing the development of the nonlinear site amplification model are given in Campbell and Bozorgnia (2007, 2008).

As discussed previously, in some applications engineers require an estimate of the aleatory uncertainty of the arbitrary horizontal component (Baker and Cornell, 2006), which is given by the equation

$$\sigma_{Arb} = \sqrt{\sigma_T^2 + \sigma_C^2} \quad (3.18)$$

where  $\sigma_C$  is defined as

$$\sigma_C^2 = \frac{1}{4N} \sum_{j=1}^N (\ln y_{1j} - \ln y_{2j})^2, \quad (3.19)$$

In the above equations,  $y_{ij}$  is the value of the ground motion parameter for component  $i$  of recording  $j$  and  $N$  is the total number of recordings. Values of  $\sigma_C$  are listed in Table 2. Also listed in this table for reference are the values of  $\sigma_T$  and  $\sigma_{Arb}$  for ground motions that are subject to linear site response (i.e., for  $V_{S30} \geq k_1$  or for small values of  $A_{1100}$ ). For ground motions subject to nonlinear site response, these standard deviations should be calculated from Eqns. 3.15–3.19 using the values listed in Table 2.

Table 2. Standard deviations for the aleatory uncertainty model

$T$ (s)	$\sigma_{\ln Y}$	$\tau_{\ln Y}$	$\sigma_C$	$\sigma_T$	$\sigma_{Arb}$	$\rho$
0.010	0.478	0.219	0.166	0.526	0.551	1.000
0.020	0.480	0.219	0.166	0.528	0.553	0.999
0.030	0.489	0.235	0.165	0.543	0.567	0.989
0.050	0.510	0.258	0.162	0.572	0.594	0.963
0.075	0.520	0.292	0.158	0.596	0.617	0.922
0.10	0.531	0.286	0.170	0.603	0.627	0.898
0.15	0.532	0.280	0.180	0.601	0.628	0.890
0.20	0.534	0.249	0.186	0.589	0.618	0.871
0.25	0.534	0.240	0.191	0.585	0.616	0.852

0.30	0.544	0.215	0.198	0.585	0.618	0.831
0.40	0.541	0.217	0.206	0.583	0.618	0.785
0.50	0.550	0.214	0.208	0.590	0.626	0.735
0.75	0.568	0.227	0.221	0.612	0.650	0.628
1.0	0.568	0.255	0.225	0.623	0.662	0.534
1.5	0.564	0.296	0.222	0.637	0.675	0.411
2.0	0.571	0.296	0.226	0.643	0.682	0.331
3.0	0.558	0.326	0.229	0.646	0.686	0.289
4.0	0.576	0.297	0.237	0.648	0.690	0.261
5.0	0.601	0.359	0.237	0.700	0.739	0.200
7.5	0.628	0.428	0.271	0.760	0.807	0.174
10.0	0.667	0.485	0.290	0.825	0.874	0.174
PGA	0.478	0.219	0.166	0.526	0.551	1.000
PGV	0.484	0.203	0.190	0.525	0.558	0.691
PGD	0.667	0.485	0.290	0.825	0.874	0.174

#### 4. CONCLUSIONS

We consider our new NGA ground motion prediction equations to be appropriate for estimating PGA, PGV, PGD and linear elastic response spectra ( $T = 0.01\text{--}10$  s) for shallow continental earthquakes occurring in western North America and other regimes of similar active tectonics such as southern Europe (Campbell and Bozorgnia, 2006; Stafford et al., 2008). The model is considered most reliable when evaluated for (1)  $M > 4.0$ ; (2)  $M < 8.5$  for strike-slip faulting,  $M < 8.0$  for reverse faulting, and  $M < 7.5$  for normal faulting; (3)  $R_{RUP} = 0\text{--}200$  km; (4)  $V_{S30} = 150\text{--}1500$  m/s or alternatively NEHRP site classes B ( $V_{S30} = 1070$  m/s), C ( $V_{S30} = 525$  m/s), D ( $V_{S30} = 255$  m/s) and E ( $V_{S30} = 150$  m/s); (4)  $Z_{2.5} = 0\text{--}10$  km; (5)  $Z_{TOR} = 0\text{--}15$  km; and (6)  $\delta = 15\text{--}90^\circ$ . As an example, the predicted attenuation and magnitude scaling characteristics of PGA and response spectra ( $M = 7.0$  and  $R_{RUP} = 10$  km, respectively) for rock with  $V_{S30} = 760$  m/s, a sediment depth of 2.5 km, and strike-slip faulting are displayed in Figs. 2 and 3.

#### ACKNOWLEDGEMENTS

This study was sponsored by the Pacific Earthquake Engineering Research Center's (PEER's) Program of Applied Earthquake Engineering Research of Lifelines Systems supported by the California Department of Transportation, the California Energy Commission, and the Pacific Gas and Electric Company. This work made use of the Earthquake Engineering Research Centers Shared Facilities supported by the National Science Foundation, under award number EEC-9701568 through PEER. Any opinions, findings, and conclusions or recommendations expressed in this material are those of the authors and do not necessarily reflect those of the National Science Foundation.

#### REFERENCES

- Baker, J.W. and Cornell, C.A. (2006). Which spectral acceleration are you using? *Earthquake Spectra* **22**, 293–312.
- Boore, D.M., Watson-Lamprey, J. and Abrahamson, N. (2006). Orientation-independent measures of ground

motion, *Bulletin of the Seismological Society of America* **96**, 1502–1511.

Chiou, B., Darragh, R., Gregor, N. and Silva, W. (2008). NGA project strong-motion database. *Earthquake Spectra* **24**, 23–44.

Campbell, K.W. (1997). Empirical near-source attenuation relationships for horizontal and vertical components of peak ground acceleration, peak ground velocity, and pseudo-absolute acceleration response spectra. *Seismological Research Letters* **68**, 154–179.

Campbell, K.W. and Bozorgnia, Y. (2003). Updated near-source ground motion (attenuation) relations for the horizontal and vertical components of peak ground acceleration and acceleration response spectra. *Bulletin of the Seismological Society of America* **93**, 314–331.

Campbell, K.W. and Bozorgnia, Y. (2006). Next generation attenuation (NGA) empirical ground motion models: can they be used in Europe?, in *Proceedings, First European Conference on Earthquake Engineering and Seismology*, Paper No. 458, Geneva, Switzerland.

Campbell, K.W. and Bozorgnia, Y. (2007). Campbell-Bozorgnia NGA ground motion relations for the geometric mean horizontal component of peak and spectral ground motion parameters, PEER Report No. 2007/02, Pacific Earthquake Engineering Research Center, University of California, Berkeley, California, USA.

Campbell, K.W. and Bozorgnia, Y. (2008). NGA ground motion model for the geometric mean horizontal component of PGA, PGV, PGD and 5% damped linear elastic response spectra for periods ranging from 0.01 to 10 s. *Earthquake Spectra* **24**, 139–171.

Power, M., Chiou, B., Abrahamson, N., Bozorgnia, Y., Shantz, T. and Roblee, C. (2008). An overview of the NGA project. *Earthquake Spectra* **24**, 3–21.

Stafford, P.J., Strasser, F.O. and Bommer, J.J. (2008). An evaluation of the applicability of the NGA models to ground-motion prediction in the Euro-Mediterranean region. *Bulletin of Earthquake Engineering* **6**, 149–177.

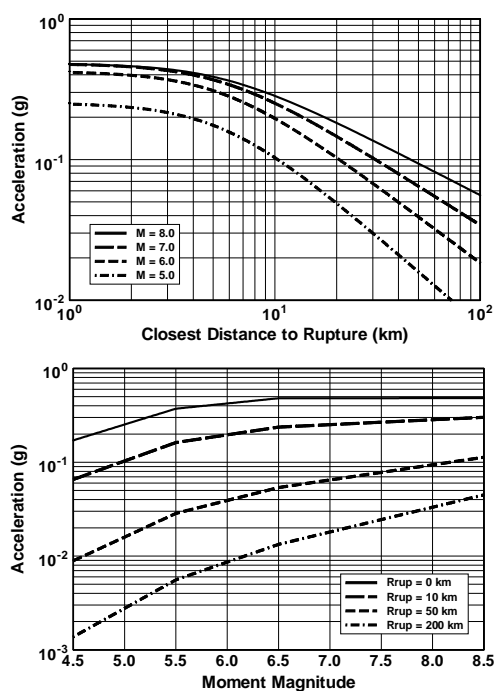


Figure 2. Predicted estimates of PGA.

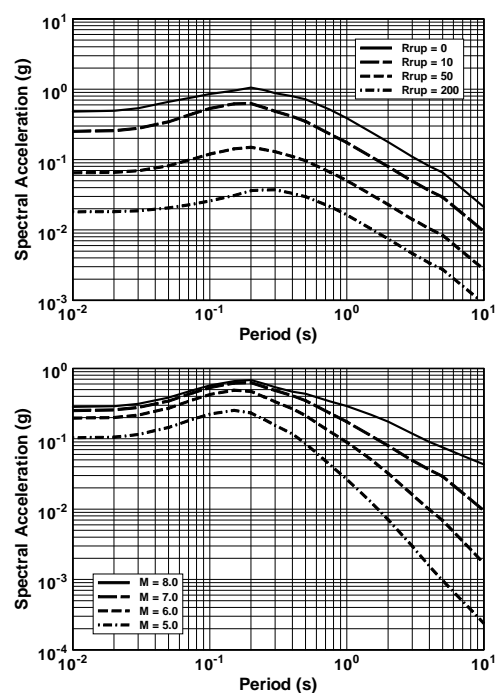


Figure 3. Predicted estimates of PSA.